# Physical Characterization of Eco-Friendly O/W Emulsions Developed Through a Strategy Based on Product Engineering Principles

**Jenifer Santos, Luis A. Trujillo-Cayado, Nuria Calero, and José Muñoz**
Reología Aplicada, Tecnología de Coloides, Dept. de Ingeniería Química, Facultad de Química, Universidad de Sevilla c/P, García González, 1, E41012, Sevilla, Spain

*DOI 10.1002/aic.14460*
*Published online April 8, 2014 in Wiley Online Library (wileyonlinelibrary.com)*

*Many traditional industrial products are being gradually replaced by environmental friendly alternatives. N,N-Dimethyldecanamide and D-limonene are solvents that fulfil the requirements to be considered green solvents and may find application in agrochemicals. This contribution deals with the study of emulsions formulated with a mixture of these solvents and an eco-friendly emulsifier. The procedure followed for the development of these formulations was based on the application of product design principles. This led to the optimum homogenization rate and subsequently to the optimum ratio of solvents. The combination of different techniques (rheology, laser diffraction, confocal laser-scanning microscopy, and multiple light scattering) was demonstrated to be a powerful tool to assist in the prediction of the emulsions destabilization process. Thus, we found that the optimum ratio of solvents was 75/25 (N,N-dimethyldecanamide/D-limonene) on account of the lack of coalescence and of a low creaming rate.* © 2014 American Institute of Chemical Engineers *AIChE J*, 60: 2644–2653, 2014

*Keywords: eco-friendly emulsions, rheology, MLS, laser diffraction, product engineering*

## Introduction

Emulsion is one of the most common formulation types for agricultural pesticides. This formulation type allows the pesticides to be easy to use, transport, and mix,[1] which contributes an added value for a new product. Traditionally, more than 25% of all pesticides contain high concentrations of organic solvents, which represent a fire hazard, may also be toxic and contribute to atmospheric volatile compound emissions.[2] Thus, many of the classical solvents are being gradually replaced by the so-called "green" solvents such as fatty acid dimethylamides (FAD) and D-limonene. FAD are solvents that fulfill the requirements to be considered green solvents and may find application in agrochemicals.[3]

D-limonene, a naturally occurring hydrocarbon, is a cyclic monoterpene, which is commonly found in the rinds of citrus fruits such as grapefruit, lemon, lime, and in particular, oranges. D-limonene exhibits good biodegradability, hence it may be proposed as an interesting alternative to organic solvents.[4,5] These solvents can meet the ever-increasing safety and environmental demands of the 21st century.

*N*,*N*-Dimethylamide is partially soluble in water, which may provokes some problems of the emulsion stability such as Ostwald ripening. A possible solution to this problem may be the addition of a second disperse phase component such as D-limonene, which is rather insoluble in the continuous phase. In addition, the presence of a surfactant helps to retard the destabilizing process and ensures long-term stability.

Ethoxylated glycerine esters are also eco-friendly and nontoxic,[6] hence their consideration as green surfactants. Their use in detergents and personal care products is disclosed in several patents.[7,8]

In order to improve the emulsions stability, it is of prime importance to detect destabilization processes at an early stage to shorten the aging test. The rheology of emulsions from both a fundamental and an applied point of view is an important tool to detect the various destabilization processes that occur in emulsions. For instance, measurements of the viscosity at very low stresses may be quite suitable in order to predict creaming.[9] Conversely, laser diffraction is the best method to characterize droplet sizes distribution (DSD) and coalescence process. Besides, the technique of multiple light scattering (MLS) is able to characterize droplet or aggregate size variation and droplet/aggregate migration as a function of aging time.[10]

This work expects to show that the combined use of different techniques such as rheology, laser diffraction, and MLS provide very interesting information at an early stage about the mechanisms of destabilization occurring in emulsions.

The main objective of this work was the study of the influence of the ratio of a mixture of green solvents (*N*,*N*-dimethyldecanamide and D-limonene) on the physical stability of slightly concentrated O/W emulsions formulated with these eco-friendly solvents and a polyoxyethylene glycerol

Correspondence concerning this article should be addressed to N. Calero at nuriacalero@us.es.

© 2014 American Institute of Chemical Engineers

ester as emulsifier. These emulsions may be used as matrices for incorporation of active agrochemical ingredients. This work is a contribution to the development of new products, which may fulfill the customers' needs as well as the related industries' requirements. This is the one of the foundations of the so-called chemical product design and engineering.[11] On top of that, the overall goal of this project is under the frame of sustainable chemical engineering insofar as applications of bio-based chemicals are explored.[12] Also, according to this principle, a specific strategy was followed considering the emulsion formulation and the reduction of energy input in order to obtain fine stable emulsions.[13]

## Materials and Methods

### *Materials*

*N*,*N* Dimethyldecanamide (Agnique AMD-10™) was kindly provided by BASF. D-Limonene was supplied by Sigma Chemical Company. The emulsifier used was a non-ionic surfactant derived from cocoa oil. Namely, a polyoxyethylene glycerol fatty acid ester, Glycereth-17 Cocoate (HLB:13), received as a gift from KAO, was selected. Its trade name is Levenol C-201™. RD antifoam emulsion (DOW CORNING®) was used as antifoaming agent. This commercial product consists of an aqueous solution containing polydimethyl siloxane (<10 %w/w) and dimethyl siloxane, hydroxyl-terminated (<10 %w/w). Deionized water was used for the preparation of all emulsions.

### *Emulsion development*

In the preliminaries studies emulsions containing 3 wt % Levenol C-201 as emulsifier, 0.1 wt % antifoam emulsion and 30 wt % solvent(s) were prepared. The ratio of solvents studied were 100/0, 75/25, 50/50, 25/75, and 0/100 of AMD-10/D-limonene. These O/W emulsions were carried out using a rotor-stator homogenizer (Silverson L5M), equipped with a mesh screen, at different homogenization rates (7000, 6000, 5000, 4000, and 3000 rpm) during 60 s.

When focusing on ratio of solvents, homogenization rate was fixed at 6000 rpm during 60 s in the emulsions with the following new AMD-10/D-limonene ratios: 65/35, 70/30, 80/20, and 85/15.

### *Interface tension measurements*

Interface tension measurements were performed with a drop pro-file analysis tensiometer (CAM200, KSV, Finland). The drop was formed inside a thermostated cuvette at 20°C and controlled using a custom-built control unit consisting of a syringe with a piston that is driven by a stepper motor. The control procedure was as follows: once the drop was formed the contour of the drop was acquired and then the drop initial area was calculated. Every 10 s the area was calculated and the actual and initial values were compared. If the values differed then the stepper motor drove the piston in the respective direction to correct the difference.

### *Droplet size distribution measurements*

Size distribution of oil droplets were determined by laser diffraction using Mastersizer X (Malvern, Worcestershire, UK). All measurements were done for three times for each emulsion. These measurements were carried out after 1, 3, 13, 21, and 40 days aging time to analyze likely coalescence effects.

The mean droplet diameter was expressed as Sauter diameter ($D_{2,3}$) and volume mean diameter ($D_{3,4}$)

$$D[M,N]=\left[\frac{\int D^M n(D)dD}{\int D^N n(D)dD}\right]^{\frac{1}{M-N}} \quad (1)$$

The uniformity is an index of polydispersity of the different droplets sizes, defined by the following expression

$$U=\frac{\sum V_i|d(v,0.5)-d_i|}{d(v,0.5)\sum V_i} \quad (2)$$

Where $d(v,0.5)$ is the median for the distribution, and $V_i$ is the volume of droplets with a diameter $d_i$.

### *Rheological measurements*

Rheological experiments were conducted with a Haake MARS controlled-stress rheometer (Thermo-Scientific, Germany), equipped with a sand-blasted coaxial cylinder Z-20 (sample volume: 8.2 mL, $Re/Ri = 1.085$, $Ri = 1$ cm) to avoid slip effects. Flow curves were carried out from 0.05 to 1 Pa at 20°C. Flow curves were carried out after 1, 3, 13, 21, and 40 days aging time to follow the effect of aging time. All measurements were repeated three times with each emulsion. Samples were taken at about 2 cm from the upper part of the container. Sampling from the top part of the container in contact with air was avoided.

Rheological measurements were carried out for the 85/15, 80/20, 75/25, 70/30, and 65/35 emulsions.

### *Multiple light scattering*

MLS measurements with a Turbiscan Lab Expert were used in order to study the destabilization of the emulsions. Measurements were carried out until 40 days at 20°C to determine the predominant mechanism of destabilization in each emulsion as well as the kinetics of the destabilization process. MLS is a sensitive and nonintrusive technique to monitor physical stability of emulsions[14,15] and more complex systems such as suspoemulsions.[16]

To characterize the creaming process, it is used the creaming index (CI)[17]

$$CI=100\cdot\frac{H_S}{H_E} \quad (3)$$

Where, $H_E$ is the total height of the emulsion and $H_S$ is the height of the serum layer.

MLS measurements in the middle zone of the vial also allowed the evolution of a mean droplet diameter with aging to be monitored.

### *Microscopic observation*

The microstructure of some emulsions was observed using a confocal laser-scanning microscope (CLSM; Leica TCS-SP2).

For CLSM microscopy, a proper amount of emulsion was placed in a test tube and subsequently Nile red solution (1 mM in DMSO) were added and mixed thoroughly. That solution is selective to the AMD solvent. The mixture was dropped on a microscope slide, which was covered with a cover slip and observed under the microscope with 100× oil

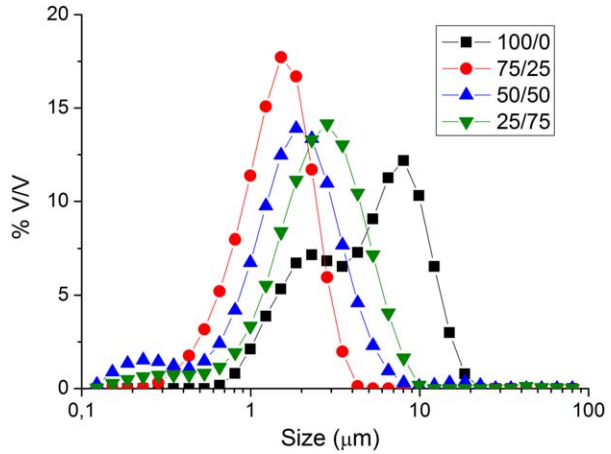


**Figure 1. Droplet size distribution for the 100/0, 75/25, 50/50, and 25/75 emulsions processed at 3000 rpm.**

**Aging time: 1 day. $T^a = 20°C$. [Color figure can be viewed in the online issue, which is available at wileyonlinelibrary.com.].**

immersion objective lens. The samples were excited at 488 nm. The emission was recorded at 500–600 nm.

## Results and Discussion

### *Exploring the composition and homogenization process*

Figure 1 shows the droplet size distribution of the emulsions with different ratios of solvents processed at the minimum speed studied (3000 rpm). This was chosen to assess if a low-energy input would yield emulsions with reasonable mean diameters and physical stability. First, it should be stated that no result for the emulsion with D-limonene as the unique solvent is shown because D-limonene could not be emulsified under this processing condition. D-Limonene is a strongly nonpolar solvent possessing a high interfacial tension (Table 1). This may be a disadvantage during the emulsification process, since lower interfacial tension results in higher ability to break into droplets.[18] Table 1 also shows the interfacial tensions of different mixtures of AMD-10/D-limonene and water. An increase in AMD-10 content of the solvent mixture provoked a progressive decrease of the interfacial tension, such that the lowest interfacial tension was reached by pure AMD-10. However, this extremely low interfacial tension led to an emulsion showing a bimodal droplet size distribution with a high polydispersity (Figure 1), that resulted in high values of the uniformity parameter (Table 2). In addition, AMD-10 is a slightly polar solvent and partially soluble in water (340 mg/L at 20°C). The use of partially water-soluble solvents (as the dispersed phase in emulsions) may specially lead to destabilization of emulsions by the Ostwald ripening phenomenon.[17,19] In addition oil droplet flocculation, creaming and coalescence may also take place.

**Table 1. Values of Interfacial Tension for Different Ratios of Solvents and Water at 20°C**

| Ratio of solvents | Interfacial tension (mN/m) |
|---|---|
| 0/100 | 40.0 ± 1.3 |
| 1/99 | 27.3 ± 0.8 |
| 5/95 | 17.5 ± 0.7 |
| 10/90 | 14.1 ± 0.7 |
| 25/75 | 7.0 ± 0.4 |
| 50/50 | 3.5 ± 0.3 |
| 75/25 | 1.6 ± 0.1 |
| 100/0 | 1.0 ± 0.1 |

Enhanced droplet size distributions were observed when both solvents were used, congruently with the controlled reduction of interfacial tensions achieved. It is worth noting that the addition of just 1 wt % of AMD-10 to D-limonene reduced interfacial tension by 33% (Table 1). This could be due to the fact that AMD-10 was able to migrate to the interface. Thus, droplets could be formed by both solvents distributed according to the solvents' concentration gradient. In this way, AMD-10 would tend to stay nearest the interface and limonene in the core of droplets, which could be similar to a "core-shell" model.[20,21]

In Figure 2a, the CI was plotted as a function of aging time at different ratios of solvents for the emulsion processed at 3000 rpm, which allowed the kinetics of the destabilization process by creaming to be analyzed and quantified.

First, it should be noted that 25/75 emulsion did not show destabilization by creaming. However, emulsions with higher AMD-10/D-limonene ratios showed a linear dependence of the CI with aging time in absence of a delay time for creaming. The slope of the linear region is directly related to the kinetics of the destabilization process, which is called the "creaming rate." The 75/25 emulsion showed lower creaming rate than both 50/50 and 100/0 emulsions (see the inset of Figure 2a).

Figure 2b shows the increase of droplet diameter from the diameter at time zero as a function of aging time for a homogenization rate of 3000 rpm.

This plot allows for detecting flocculation and/or coalescence phenomena. On the one hand, an increase of droplet size over time was detected for the 50/50 and 25/75 emulsions. Conversely, the emulsions without D-limonene or with lower contents of this (100/0 and 75/25) did not undergo these destabilization phenomena as demonstrated by the fact that droplet diameter did not show any significant changes with aging time.

**Table 2. Values of Sauter Diameter and Uniformity for All Emulsions Studied**

| | Homogenization rate (rpm) | | | | | | | | | |
|---|---|---|---|---|---|---|---|---|---|---|
| | 7000 | | 6000 | | 5000 | | 4000 | | 3000 | |
| Ratio of solvents | $D_{2,3}$ (μm) | uniformity ($10^{-1}$) | $D_{2,3}$ (μm) | uniformity ($10^{-1}$) | $D_{2,3}$ (μm) | uniformity ($10^{-1}$) | $D_{2,3}$ (μm) | uniformity ($10^{-1}$) | $D_{2,3}$ (μm) | uniformity ($10^{-1}$) |
| 100/0 | 2.72 | 5.70 | 3.09 | 7.29 | 1.78 | 3.93 | 3.42 | 4.68 | 3.75 | 6.02 |
| 75/25 | 0.33 | 9.26 | 0.35 | 7.54 | 0.47 | 7.18 | 0.73 | 4.34 | 1.07 | 3.79 |
| 50/50 | 0.27 | 11.01 | 0.29 | 9.68 | 0.34 | 8.72 | 0.64 | 7.80 | 1.05 | 5.16 |
| 25/75 | 0.6 | 9.87 | 0.72 | 8.87 | 1.02 | 7.17 | 1.57 | 4.53 | 1.55 | 4.96 |
| 0/100 | 1.83 | 3.77 | 2.43 | 4.10 | 2.50 | 5.03 | 3.15 | 4.57 | – | – |

Standard deviation of the mean (three replicates) for $D^{2,3} < 5\%$.
Standard deviation of the mean (three replicates) for uniformity $< 5\%$.

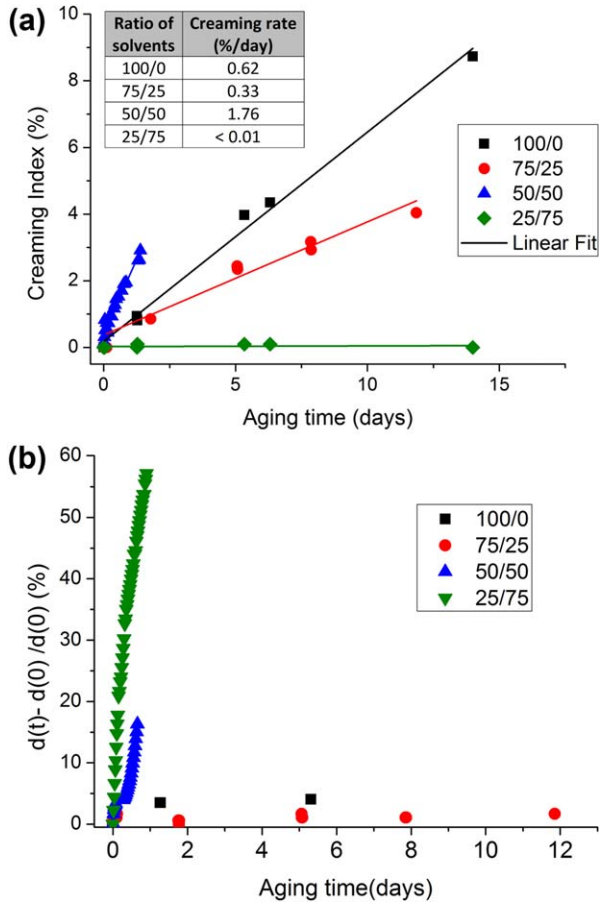


**Figure 2. (a) CI as a function of the aging time for emulsions processed at 3000 rpm; (b) increase of droplet diameter from the diameter at time zero as a function of aging time for a homogenization rate of 3000 rpm.**

**For (a), samples kept under storage at 20°C. Note: the data for 50/50 composition is not shown for aging time later than 3 days since emulsion phase separation occurred. It precludes further creaming measurements. For (b), samples kept under storage at 20°C. [Color figure can be viewed in the online issue, which is available at wileyonlinelibrary.com.]**

An overall analysis of the MLS results allows us to conclude that although the 25/75 emulsion showed the best results against destabilization by creaming, it underwent immediate destabilization by flocculation and/or coalescence. However, it is important to clarify that MLS technique does not distinguish by itself between flocculation and coalescence since both mechanisms provoke in this case an increase of backscattering in the middle zone of the measuring cell. By contrast, creaming process involves a decrease of backscattering in the low zone of the measuring cell, although this was not observed. In addition, creaming was not detected by naked eye. A tentative explanation may be that that creaming is covered up by flocculation and/or coalescence.

Hence, the 75/25 emulsion showed the best physical stability results for the homogenization rate of 3000 rpm.

On account of the poor results obtained with the lowest energy input provided by 3000 rpm homogenization rate, this was increased up to 7000 rpm. Sauter diameter and uniformity values obtained at 4000, 5000, 6000, and 7000 rpm are shown in Table 2. Figure 3 shows by way of example

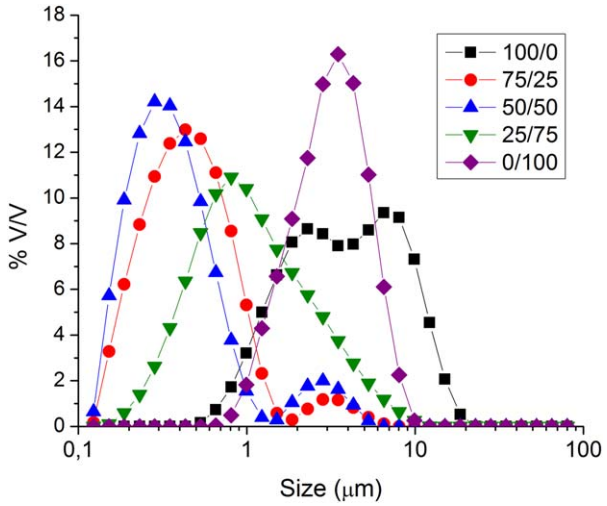


**Figure 3. Droplet size distribution for the emulsions processed at 6000 rpm.**

**Aging time: 1 day. $T = 20°C$. [Color figure can be viewed in the online issue, which is available at wileyonlinelibrary.com.]**

the droplet size distributions of emulsions prepared with different ratios of solvents and processed at 6000 rpm.

It was observed that the use of pure solvents yielded macroemulsions with Sauter mean diameters above 1 $\mu$. However, the use of solvent mixtures caused a decrease of droplet size to submicron values (Table 2). Furthermore, the ratio of solvents determined the final size distribution of the emulsion. Thus, the lower Sauter diameters were found for 50/50 emulsions, 270 nm being the lowest value reached. Despite this, it should be noted that higher contents of AMD-10 provoked bimodal distributions with a second population above 1 $\mu$ (centered around 3 $\mu$). The occurrence of the second population of droplets may be related to a recoalescence phenomenon induced by an excess of mechanical energy input during the emulsification process. Recoalescence phenomenon is due to the fact that emulsion droplets are subjected to excessive kinetic energy as a result of high-intensity turbulence in emulsification systems, which in turn yields the partial rupture of the interface of some droplets.[22] This is consistent with the fact that the appearance of this second peak occurred only for emulsions processed above 5000 rpm.

The lower values of the Sauter mean droplet size obtained for 50/50 emulsions for all homogenization rates studied were counterbalanced by the lower polydispersity of emulsions with the ratio of solvents at 75/25, as indicated by the uniformity values obtained. McClements stated that an increase of polydispersity determines the stability of the emulsion as it provokes an increase of creaming rate due to higher values of the effective packing parameter.[23]

In Figure 4a, the CI was plotted as a function of aging time at different ratios of solvents for emulsions processed at 6000 and 7000 rpm.

The 75/25 emulsion showed a slower creaming rate and greater delay time for creaming for both homogenization rates (see the inset of Figure 4a). This fact indicates that emulsions with this ratio of solvents exhibited better physical stability against creaming as the results for emulsion processed at 3000 rpm had already pointed. However, the emulsions processed at 6000 and 7000 rpm showed greater delay time for creaming and lower rate of creaming than those

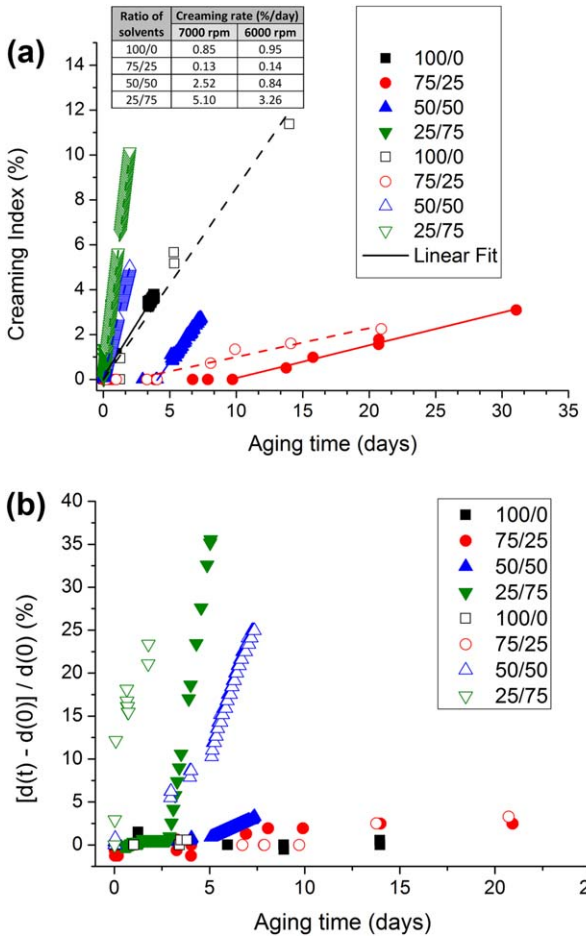


**Figure 4. (a) CI as a function of aging time for the emulsions 100/0, 75/25, 50/50, and 25/75 processed at 6000 rpm (closed symbols) and 7000 rpm (open symbols); (b) increase of droplet diameter from the diameter at time zero as a function of aging time for emulsions 100/0, 75/25, 50/50, 25/75 processed at 6000 rpm (closed symbols) and 7000 rpm (open symbols).**

**For (a), continuous lines illustrate data fitting to a linear fit for the emulsions processed at 6000 rpm and dash illustrate data fitting to a linear fit for the emulsions processed at 7000 rpm. [Color figure can be viewed in the online issue, which is available at wileyonlinelibrary.com.]**

processed at 3000 rpm (see Figures 2a and 3). This is related to larger droplet sizes favoring destabilization by creaming.[17] In addition, the emulsion processed at 6000 rpm showed higher delay time for creaming than that processed at 7000 rpm. The latter emulsion was slightly overprocessed since it showed a more noticeable second peak in DSD (recoalescence), which resulted in a higher uniformity value (Table 2).

Figure 4b shows the relative increase of droplet diameter from the diameter at time zero as a function of aging time for homogenization rates of 6000 and 7000 rpm.

First, it should be noted that both 25/75 and 50/50 emulsions underwent an increase of droplet size with aging time caused by flocculation and/or coalescence. In contrast, the 100/0 and 75/25 emulsions processed at both homogenization rates (6000 and 7000 rpm) did not exhibit destabilization by flocculation and/or coalescence for the test time.

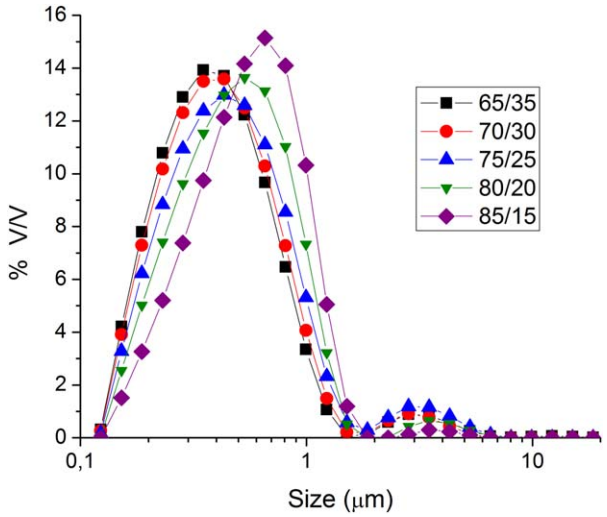


**Figure 5. Droplet size distribution of 65/35, 70/30, 75/25, 80/20, and 85/15 emulsions.**

**Aging time: 1 day. $T = 20^{\circ}$C. [Color figure can be viewed in the online issue, which is available at wileyonlinelibrary.com.]**

Taking into account the above results, we concluded that the emulsion formulated with a 75/25 ratio of solvents and prepared at 6000 rpm provided the best stability results for the test time. For this reason, it was taken as a starting point for further analysis for optimizing the formulation.

### *Focusing on ratio of solvents*

Figure 5 shows the DSD of emulsions with different solvent ratios, around the 75/25 value, processed at 6000 rpm.

All emulsions studied showed bimodal distributions with the majority of the population below 1 $\mu$ and a second peak at higher sizes as a consequence of the aforementioned recoalescence phenomenon induced by an excess of mechanical energy-input. Moreover, an increase of the AMD-10 content provoked the distributions to shift toward greater droplet sizes. Table 3 shows the values of the Sauter and volumetric mean diameters ($D_{2,3}$ and $D_{3,4}$). Sauter mean diameter values ranged from 0.31 to 0.42 $\mu$m and volumetric mean diameters varied between 0.48 and 0.57 $\mu$m.

Figure 6 shows the flow properties for 1-day-aged emulsions studied as a function of the ratio of solvents. All the emulsions exhibited a trend to reach a Newtonian region at low-shear rate regime, which is defined by the zero-shear viscosity, ($\eta_0$). This range is followed by a slight decrease in viscosity (shear-thinning behavior) above a critical shear

**Table 3. Sauter and Volumetric Mean Diameters for 65/35, 70/30, 75/25, 80/20, and 85/15 Emulsions**

| Ratio of solvents | $D_{2,3}$ ($\mu$m) | $D_{3,4}$ ($\mu$m) |
|---|---|---|
| 65/35 | 0.31 | 0.50 |
| 70/30 | 0.32 | 0.48 |
| 75/25 | 0.35 | 0.57 |
| 80/20 | 0.37 | 0.54 |
| 85/15 | 0.42 | 0.57 |

Standard deviation of the mean (three replicates) for $D^{2,3} < 4\%$.
Standard deviation of the mean (three replicates) for $D^{3,4} < 6\%$.

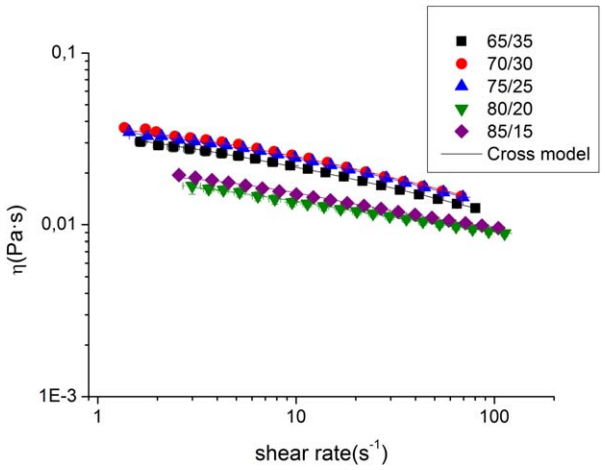


**Figure 6. Flow curves for the studied emulsions as a function of ratio of solvents for 1 day aging time at 20°C.**

**Continuous lines illustrate data fitting to the Cross model. [Color figure can be viewed in the online issue, which is available at wileyonlinelibrary.com.]**

rate. Figure 6 also illustrates the fitting quality of the results obtained to the Cross model ($R^2 > 0.999$)

$$\eta = \frac{\eta_0}{1 + \left(\frac{\dot{\gamma}}{\dot{\gamma}_c}\right)^{1-n}} \tag{4}$$

$\dot{\gamma}_c$ is related to the critical the shear rate for the onset of shear-thinning response, $\eta_0$ stands for the zero-shear viscosity and $(1-n)$ is a parameter related to the slope of the power-law region; $n$ being the so-called flow index. For shear thinning materials, $0 < n < 1$. A solid material would show $n = 0$, while a Newtonian liquid would show $n = 1$.

The values of these parameters are shown in Table 4 as a function of the ratio of solvents. Zero-shear viscosity of the three emulsions studied with higher limonene content showed no significant differences. However, two levels of zero-shear viscosity values were observed, 75/25 being the key ratio of solvents. In fact, a stepwise decrease in zero-shear viscosity with ratio of solvents was observed from 75/25 to 80/20 and 80/15 emulsions. This is consistent with the slightly higher Sauter diameters found for the high AMD-10 content emulsions. Conversely, the higher zero-shear viscosities of emulsions with a solvent ratio lower than 75/25 may be attributed to the slightly lower Sauter diameters as well as to a flocculation process leading to the onset of some creaming for emulsions aged for 1 day. Greater tendency to flocculate has been previously associated to finer emulsions by Pal and Barnes.[24,25]

**Table 4. Flow Curves Fitting Parameters for the Cross Model for Studied Emulsions as a Function of Ratio of Solvents at 1 Day of Aging Time**

| Ratio of solvents | $\eta_0$ (Pa·s) | $\dot{\gamma}_c$ ($s^{-1}$) | $1-n$ |
|---|---|---|---|
| 65/35 | 0.053 | 3.12 | 0.43 |
| 70/30 | 0.053 | 7.82 | 0.43 |
| 75/25 | 0.050 | 8.73 | 0.43 |
| 80/20 | 0.034 | 1.27 | 0.41 |
| 85/15 | 0.034 | 3.12 | 0.41 |

Standard deviation of the mean (three replicates) for $\eta_0 < 10\%$.
Standard deviation of the mean (three replicates) for $\dot{\gamma}_c < 10\%$.
Standard deviation of the mean (three replicates) for $1-n < 10\%$.

These authors attributed the trend to the flocculation to two different mechanisms: the occurrence of Brownian motion between droplets, and the fact that the droplets are subject to dominant Van der Waals attraction forces. This interpretation is strengthened by the fact that no significant differences of DSD obtained by laser diffraction were found. This may be explained by taking into account that weakly flocculated droplets are likely disrupted due to dilution and stirring during measurement carried out by laser diffraction.[26]

Figure 7 shows the CLSM micrographs obtained for the 75/25 emulsion.

Droplet sizes observed are consistent with the results obtained by laser diffraction. Moreover, micrographs reveal the existence of flocs as commented in the previous section. It should be noted that all the droplets are stained with a fluorophore selective for AMD-10 solvent. This points out that the dispersed phase consisted of a mixture of both solvents.

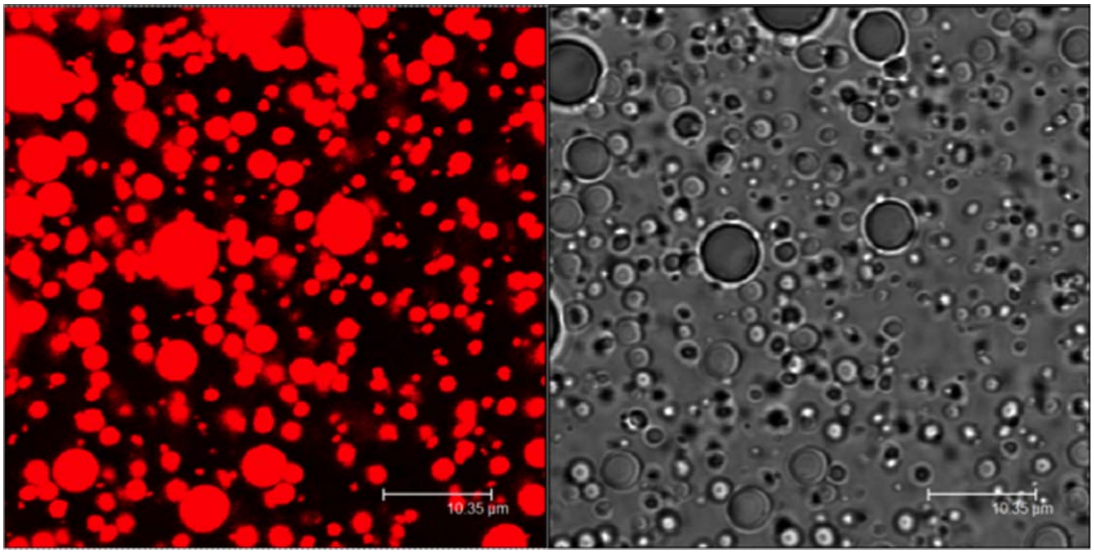


**Figure 7. CLSM microphotographs for emulsion 75/25 at 1 day of aging time.**

**[Color figure can be viewed in the online issue, which is available at wileyonlinelibrary.com.]**

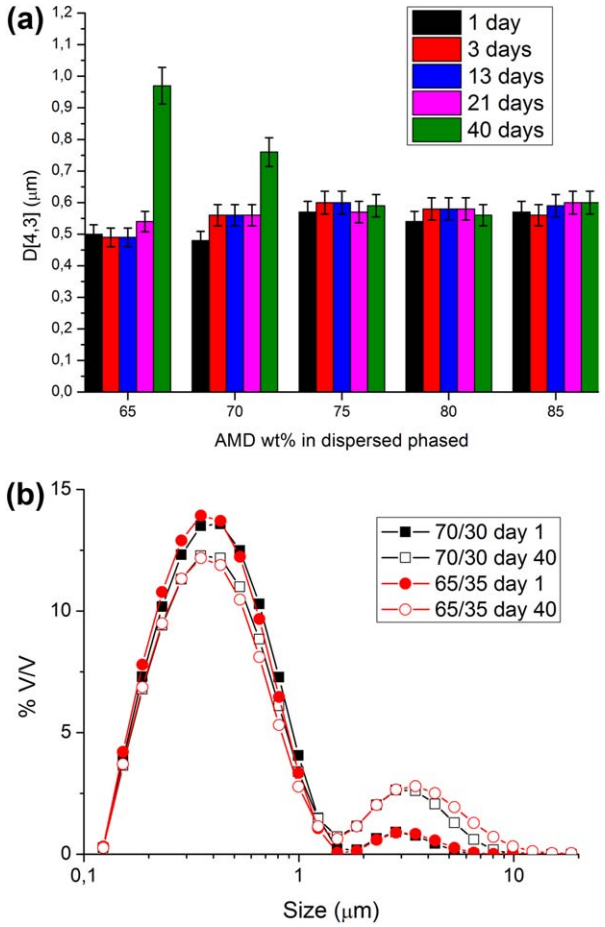


**Figure 8. (a) Volumetric mean diameter as a function of aging time for the emulsions 65/35, 70/30, 75/25, 80/20, and 85/15; (b) droplet size distributions for the emulsions 65/35 and 70/30 at 1 day and 40 days after preparation; Emulsions kept under storage at 20°C.**

**[Color figure can be viewed in the online issue, which is available at wileyonlinelibrary.com.]**

However, this does not exclude the fact that there may be a concentration gradient within the droplet, as previously explained.

Figure 8a shows the volumetric mean diameter as a function of both the ratio of solvents and aging time.

Palazolo et al.[26] previously stated that the volumetric mean diameter allows for detecting coalescence and the flocculation process with more sensitivity than the Sauter mean diameter. Thus, the 85/15, 80/20, and 75/25 emulsions did not show any significant changes of droplet sizes. By contrast, for emulsions containing less AMD-10, substantial changes of droplet size were observed, increasing by 94% for the 65/35 emulsion and by 58% for the 70/30 emulsion. This increase may indicate the existence of a destabilization phenomenon or coalescence by Ostwald ripening. The increase of volumetric mean diameter with time cannot be attributed to a flocculation process, since flocs are disrupted under the action of stirring and pumping during laser diffraction measurement.

Figure 8b shows the droplet size distributions for the 65/35 and 70/30 emulsions at 1 day and 40 days after preparation.

These distributions allow an increase of the second peak with ageing time to be detected, which resulted in a reduction of the population with smaller size. This usually points to the occurrence of a destabilization process by coalescence discarding an Ostwald ripening phenomenon, as the latter would lead to a shift of the DSD toward larger sizes without changing their shape. For Ostwald ripening the particle size distribution should attain a specific time-independent form that moves up the size axis with time, whereas with coalescence a bimodal distribution is usually observed.[17,27]

Figures 9a–e show the flow curves as a function of ageing time for all emulsions studied.

All emulsions exhibited a trend to reach a Newtonian region at low-shear rate regime, followed by a slight decrease in viscosity (shear-thinning behavior) above a critical shear rate. This behavior could be fairly well fitted to the Cross model with a $R^2$ greater than 0.999. The fitting parameters are shown in the tables inset in the figures. The 65/35 emulsion showed a steady decrease in zero-shear viscosity with aging time, which is a clear indication of coalescence as confirmed by the significant increase of volumetric mean diameter from 21 ageing days on (Figures 8a and 9a). The decrease of zero-shear viscosity with time has been previously to an increase of average droplet size.[23] A slight increase of AMD-10/D-limonene ratio to 70/30 initially provoked an incipient creaming effect as demonstrated by the rise of both zero-shear viscosity and shear-thinning slope.[28] After that, coalescence became dominant as revealed by the steady drop of zero-shear viscosity at longer ageing times (Figure 9b).

An increase of zero-shear viscosity was also detected for the 75/25, 80/20, and 85/15 emulsions as shown in Figures 9c–e, respectively. The increase of zero-shear viscosity with aging time indicates a higher concentration of the dispersed phase in the upper part of the sample. This involves a destabilization process by incipient creaming and/or flocculation.

Figure 10a shows the CI as a function of aging time at different ratios of solvents. It should be noted that the slope of the linear region, directly related to the "creaming rate," was not significantly different for all studied systems (see the inset of Figure 10a). However, important changes of the delay time were found, in such a way that the most D-limonene-concentrated emulsions showed the higher values of that parameter. This is totally consistent with the result obtained from the different rheological and laser diffraction measurements.

Figure 10b shows the increase of droplet diameter from the diameter at time zero plotted as a function of ageing time for emulsions with the different ratios of solvents studied.

No changes of droplet size emulsions associated with a coalescence phenomenon were detected for emulsions with less limonene content. By contrast, emulsions with higher limonene content exhibited significant changes of droplet size as a consequence of a destabilization process by coalescence. These results are consistent with results obtained in flow curves and laser diffraction. In spite of that MLS is not able to differentiate between both coalescence and flocculation phenomena. As a result, the results obtained from the rest of the experimental techniques used reveal that changes of backscattering in the intermediate zone of the vial are essentially due to a coalescence phenomenon. It should be noted that this phenomenon is more pronounced in the emulsion with higher limonene content. This may be related to

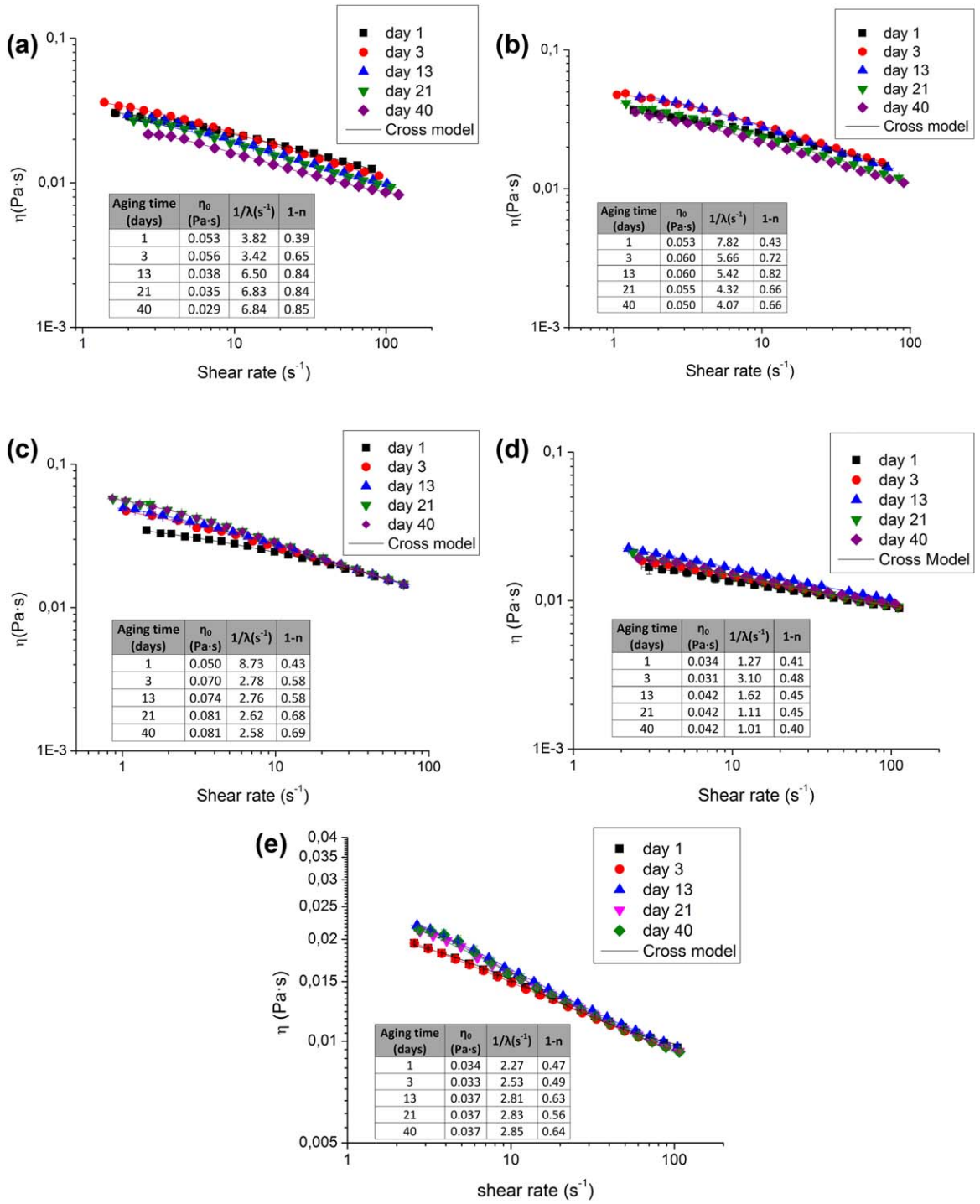


**Figure 9. Flow curves as a function of aging time for (a) 65/35, (b) 70/30, (c) 75/25, (d) 80/20, and (e) 85/15 emulsion.**

**Continuous line illustrates data fitting to the Cross model. Tables inset show the flow curve fitting parameters. [Color figure can be viewed in the online issue, which is available at wileyonlinelibrary.com.]**

the interfacial properties of limonene and its behavior at the interface.

## Conclusions

The exploring analysis initially carried out showed the dependence of homogenization rate and the ratio of solvents on DSDs and emulsion stability. The use of mixtures of green solvents led to obtain emulsions with submicron droplet mean diameter above 5000 rpm. In addition, the results of this preliminary study allowed an adequate homogenization rate to be fixed (6000 rpm) and laid the foundation for a further study of ratio of solvents. As a result of this study, an evolution of DSDs consistent with the occurrence of some coalescence was observed for emulsions with the higher content in D-limonene. However, emulsions containing high AMD-10/D-limonene ratio remained stable against coalescence. Coalescence information obtained by laser

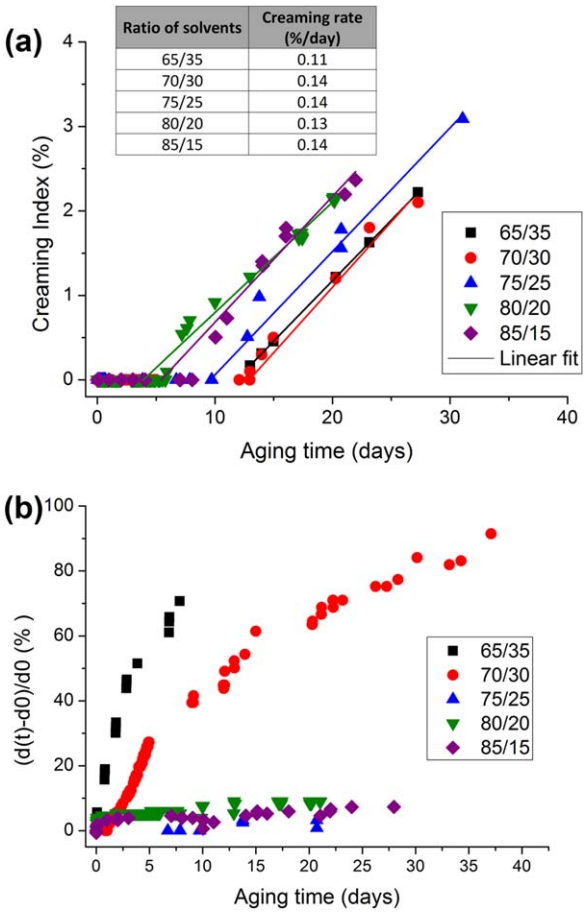


**Figure 10. (a) CI as a function of aging time for studied emulsions; (b) increase of droplet size diameter from the diameter at time zero as a function of aging time for studied emulsions.**

**[Color figure can be viewed in the online issue, which is available at wileyonlinelibrary.com.]**

diffraction and MLS supported each other. In addition, the results provided by MLS revealed that 65/35 and 70/30 emulsions underwent not only coalescence but also creaming. Emulsion with 75/25 solvent ratio exhibited intermediate delay time for the onset of incipient creaming but it did not undergo coalescence. Rheology cleared up the destabilization mechanism for high-limonene content emulsions. First, creaming was dominant (increasing $\eta_0$) and later coalescence became predominant (decreasing $\eta_0$). From a methodological point of view, monitoring the cooperative information provided by rheology, laser diffraction, MLS and CSLM for a short-aging time is a powerful tool to get a comprehensive panoramic view of the destabilization mechanism and kinetics of emulsions, especially when several mechanisms are simultaneously taking place.

## Acknowledgments

The financial support received (Project CTQ2011-27371) from the Spanish Ministerio de Economía y Competitividad, the European Commission (FEDER Programme) and from V Plan Propio Universidad de Sevilla is kindly acknowledged. The authors are also grateful to BASF and KAO for providing materials for this research.

## Notation

$D(3,2)$ = Sauter's mean diameter, $\mu$m
$D(4,3)$ = volumetric mean diameter, $\mu$m
$Re$ = radius outside cylinder (interior radius of the beaker), cm
$Ri$ = radius interior cylinder (outside radius of the rotor), cm
CI = creaming index, %
$H_s$ = total height of the emulsion, mm
$H_E$ = height of the serum layer. mm
$\eta$ = shear rate viscosity, Pa·s
$\eta_0$ = zero-shear rate viscosity, Pa·s
$\dot{\gamma}$ = shear rate, $s^{-1}$
$\dot{\gamma}_c$ = critical shear rate, $s^{-1}$
$n$ = flow index,
$\lambda$ = characteristic time, s

## Literature Cited

1. Hill RL. Detergents in agrochemical and pesticide applications. In: Zoller U, editor. Handbook of Detergents Part E: Applications. Boca Raton: Taylor & Francis Group, 2009:302–329.
2. Hofer R, Bigorra J. Green chemistry—a sustainable solution for industrial specialties applications. *Green Chem.* 2007:9;203–212.
3. Bigorra J. Innovative solvents based on renewable raw materials. In: Proceedings of 40th Annual Meeting of CED. Barcelona, Spain, 2010.
4. Medvedovici A, Udrescu S, David V. Use of a green (bio) solvent—limonene—as extractant and immiscible diluent for large volume injection in the RPLC-tandem MS assay of statins and related metabolites in human plasma. *Biomed Chromatogr.* 2012;27:48–57.
5. Walter J. Metabolism of terpenoids in animal models and humans. In: Husnu Can Baser K, Buchbauer G, editors. Handbook of essential oils: Science, Technology and Applications. Boca Raton: CRC Press, 2010:209–232.
6. Castán P, González X. Skin properties of glycerine polyethoxylene esters. In: Proceedings of 40th Annual Meeting of CED, Vol. 33. 2003:325–338.
7. Lutz PJ. Ca. Patents Applications.CA 2537554 A1 20060822, 2006.
8. Denolle Y, Seita V, Delaire V. European Patents and Applications. EP 2368971 A1 20110928, 2011.
9. Tadros ThF. Rheology of Dispersions. Principles and Applications. Weinheim, Germany: Wiley-VCH, 2010.
10. Mengual O, Meunier G, Cayré I, Puech K, Snabre P. TURBISCAN MA 2000: multiple light scattering measurement for concentrated emulsion and suspensión instability analysis. *Talanta.* 1999;50:445–456.
11. Cussler EL, Moggridge GD. Chemical Product Design, 2nd ed. Cambridge, UK: Cambridge University Press, 2011.
12. Brökel U. Meier W. Wagner G. Introduction. In: Brökel U. Meier W. Wagner G, editors. Product Design and Engineering. Vol. 1: Basics and Technologies. Weinheim: Wiley-VCH, 2007:1–3.
13. Cuéllar I, Bullóna J, Forgarini AM, Cárdenas A, Briceño MI. More efficient preparation of parenteral emulsions or how to improve a pharmaceutical recipe by formulation engineering. *Chem Eng Sci.* 2005;60:2127–2134.
14. Allende D, Cambiella A, Benito JM, Pazos C, Coca J. Destabilization-enhanced centrifugation of metalworking oil-in-water emulsions: effect of demulsifying agents. *Chem Eng Technol.* 2008;31:1007–1014.
15. Camino NA, Sanchez CC, Patino JMR, Pilosof AMR. Hydroxypropylmethylcellulose-beta-lactoglobulin mixtures at the oil-water interface. Bulk, interfacial and emulsification behavior as affected by pH. *Food Hydrocoll.* 2012;27:464–474.
16. Santos J, Trujillo LA, Calero N, Alfaro MC, Muñoz J. Physical characterization of a commercial suspoemulsion as a reference for the development of suspoemulsions. *Chem Eng Technol.* 2013;11:1–9.
17. McClements DJ. Critical review of techniques and methodologies for characterization of emulsion stability. *Crit Rev Food Sci Nutr.* 2007;47:611–649.
18. Dickinson E. Hydrocolloids at interfaces and the influence on the properties of dispersed systems. *Food Hydrocoll.* 2003;17:25–39.
19. Tadros ThF. Emulsion Science and Technology. Weinheim, Germany: Wiley-VCH, 2009.
20. Lee JM, Lim KH. Electroconductometric determination of completely engulfing Maxwell type three phase emulsions. *J Ind Eng Chem.* 2003;9:248–253.

21. Pal R. Rheology of Particulate Dispersions and Composites. Boca Raton: CRC Press, 2007.
22. Jafari SM, He Y, Bhandari B. Re-coalescence of emulsion droplets during high-energy emulsification. *Food Hydrocoll*. 2008;22:1191–1202.
23. McClements DJ. Food Emulsions: Principles, Practice, and Techniques. Boca Raton: CRC Press, 2005.
24. Pal R. Effect of droplet size on the rheology of emulsions. *AICHE J*. 1996;92:3181–3190.
25. Barnes HA. Rheology of emulsions- a review. *Coll Surface A*. 1994; 91:89–95.
26. Palazolo GG, Sorgentini DA, Wagner JR. Coalescence and flocculation in o/w emulsions of native and denatured whey soy proteins in comparison with soy protein isolates. *Food Hydrocoll*. 2005;19:595–604.
27. Weers JG. Ostwald ripening in emulsions. In: Binks BP, editor. Modern Aspects of Emulsions Science, Cambridge, UK: RSC Press. 1998:292–327.
28. Calero N, Muñoz J, Cox P W, Heuer A, Guerrero A. Influence of chitosan concentration on the stability, microstructure and rheological properties of O/W emulsions formulated with high-oleic sunflower oil and potato protein. *Food Hydrocoll*. 2013;30: 152–162.

*Manuscript received Nov. 5, 2013, revision received Jan. 24, 2014, and final revision received Mar. 28, 2014.*